

### **The Stability of an Inviscid Liquid Sheet Containing Vapor Bubbles**

Layachi Hadji, Associate Professor, Department of Mathematics, The University of Alabama,  
lhadji@bama.ua.edu

Willard Schreiber, Associate Professor, Mechanical Engineering Department, The University of Alabama,  
schreiber@eng.ua.edu

#### **Abstract**

The development of a liquid spray exiting a nozzle begins with the breakup of a liquid jet or sheet injected into a gas. The presence of vapor bubbles in a liquid jet can modify the instabilities, such as the Kelvin-Helmholtz interface instability, which causes a liquid jet or sheet to break up into a dispersion of small liquid droplets. A previously derived model is used in the present paper to investigate the influence of the presence of bubbles on the Kelvin-Helmholtz instability of an inviscid liquid sheet. It is predicted that the presence of bubbles would yield smaller liquid droplets.

#### **Introduction**

The process of a liquid jet breaking into a spray is a critical feature of many engineering applications, including fuel injection in engines and turbines, spray painting processes, and ink jet printing. Sprays formed from a liquid round jet or rectangular sheet emanating from a nozzle are particularly germane to combustion applications which inevitably incorporate diffusion-controlled mixing and combustion of liquid fuels. Understanding the physics of a combustor's fuel spray evolution is necessary for predicting the subsequent combustion process associated with heat release and emissions production for turbines, reciprocating engines, furnaces and boilers.

The well known Kelvin-Helmholtz instability describes the destabilization of the liquid-gas interface at the free surface of a thin liquid sheet moving relative to a surrounding gas. Extensive investigations of these instabilities have improved the understanding of how an initially planar liquid sheet breaks down into droplets under the action of an interfacial shear. A question of long-standing interest to engineers researching liquid sheet atomization is the effect of hydrodynamic conditions on droplet size.

The majority of the theoretical stability investigations of both the planar liquid sheet and the round jet have been linear. (See, for example, the review and analysis of Senecal et al [1].) These studies reveal that instabilities arise due to competing forces between the stabilizing influence of surface tension and viscosity and the destabilizing effect of the imposed shear stress. The density ratio of the liquid sheet and the ambient gas also affects the threshold values for instability. Linear stability studies demonstrate that the planar sheet exhibits instability as either a sinuous mode or a varicose mode. The former, being anti-symmetric, is associated with a constant liquid thickness, while the latter, being symmetrical, is characterized by alternating thin and thick regions of liquid.

Vapor bubbles, which can arise in the liquid jet leaving the nozzle as a result of cavitation of a liquid within the nozzle, increase the jet's instability in part due to the two-phase mixture's compressibility. Brennen [2] demonstrates the extent of this compressibility effect theoretically as illustrated for a water and air mixture. The speed of sound in water at 20°C decreases from around 1500 m/s for pure water to about 25 m/s in a water mixture containing a 20% volume fraction of air at atmospheric pressure. Experimental data from Karplus [3] and Gouse and Brown [4] closely match Brennen's prediction.

The hydrodynamic stability of fluid flows containing air bubbles, so-called bubbly fluids, has not attracted much attention from the research community due primarily to the complexity that the bubbles add to the model [5]. Kogarko [6], Lordanski [7], and van Wijngaarden [8] have developed a simple mathematical

model to describe the velocity and pressure fields in an inviscid liquid containing a small volume fraction in bubbles. While the liquid phase is incompressible, compressibility effects arise in the fluid solely due to the presence of the bubbles, which are assumed to be small, of a spherical shape, and to consist of a perfect gas. These bubbles, moreover, experience no slip with the moving fluid and do not interact with each other. The model is described by a single velocity field even though the system consists of two phases.

In this paper, we analyze the effect of compressibility on the stability of a fluid sheet that includes a small volume fraction of vapor. Linear equations are formulated that describe the effect that surface tension and momentum have on this inviscid fluid sheet. Surface tension acts at the interface between the liquid phase and the outside air. The surface tension at the bubbles' surfaces as well as gravity effects are negligibly small and thus are neglected. The results illustrate the effect of compressibility on the neutral stability curves as a function of the Weber number, wave number, and density ratio.

The model used in this paper is attributable to Kogorko [6], Lordanski [7], and van Wijngaarden [8] and accounts for the presence of a gas phase surrounding the moving bubbly liquid sheet. The Weber number, which describes the ratio of inertial to surface tension forces, the ratio of gas and liquid density, and the speed of sound in the liquid mixture constitute the parameters which govern the problem of bubbly liquid break up. When bubble concentration in the liquid is increased slightly above zero, the sound of speed decreases sharply. A complex dispersion relation is derived, the analysis of which demonstrates that the presence of bubbles in the liquid does not modify the threshold for the onset of the Kelvin-Helmholtz instability. The instability onset occurs at a zero Weber number, with or without the presence of bubbles; however, the presence of a minute amount of bubbles in the liquid can drastically alter the critical wavenumber. More precisely, it is found that the critical wavenumber increases with the concentration level of bubbles in the liquid. If the initial size of the droplets in the spray following breakup is correlated with the critical wavelength, our findings imply that the presence of bubbles would cause smaller liquid droplets.

## Formulation

An inviscid liquid sheet, moving with a velocity  $U_0$ , contains a small volume fraction of spherical bubbles, the concentration of which is conserved. The bubbles are assumed not to interact with each other and have no interphase velocity relative to the liquid phase. The mixture is viewed as a continuous medium with the liquid phase making up its mass and the vapor content accounting for its compressibility [8].

In this transient, two-dimensional model,  $\rho(x, z, t)$ ,  $p(x, z, t)$  and  $u(x, z, t)$  denote the average density, pressure, and velocity. Then the fluid flow in the mixture is described by the equations of mass and momentum conservation.

$$\frac{\partial \rho}{\partial t} + \frac{\partial(\rho u)}{\partial x} + \frac{\partial(\rho w)}{\partial z} = 0 \quad (1)$$

$$\rho \left( \frac{\partial u}{\partial t} + u \frac{\partial u}{\partial x} + w \frac{\partial u}{\partial z} \right) = - \frac{\partial p}{\partial x} \quad (2)$$

$$\rho \left( \frac{\partial w}{\partial t} + u \frac{\partial w}{\partial x} + w \frac{\partial w}{\partial z} \right) = - \frac{\partial p}{\partial z} \quad (3)$$

The pressures in the liquid and vapor phases are related by

$$p_g(R) = p_o \left( \frac{R_o}{R} \right)^{3\gamma} \quad (4)$$

and

$$p_g - p = \rho_l \left( R \frac{d^2 R}{dt^2} + \frac{3}{2} \left( \frac{dR}{dt} \right)^2 \right) \quad (5)$$

where  $\rho_g$  and  $\rho_l$  are the densities of the vapor and liquid phases,  $P_o$  is the equilibrium pressure, and  $\gamma$  is the polytropic gas exponent. The density of the mixture is given by

$$\rho = \left( 1 - \frac{4}{3} \pi R^3 N \right) \rho_l + \frac{4}{3} \pi R^3 N \rho_g \quad (6)$$

where  $N(x,z,t)$  and  $R(t)$  represent the number of bubbles per unit volume and the average bubble's radius, and the number  $N$  of bubbles is conserved.

The two-dimensional liquid sheet is bounded above and below by infinite layers of gas. On assuming that the latter is inviscid and incompressible, the gas flow is described by

$$\frac{\partial(u_a)}{\partial x} + \frac{\partial(w_a)}{\partial z} = 0 \quad (7)$$

$$\rho_a \left( \frac{\partial u_a}{\partial t} + u_a \frac{\partial u_a}{\partial x} + w_a \frac{\partial u_a}{\partial z} \right) = - \frac{\partial p_a}{\partial x} \quad (8)$$

$$\rho_a \left( \frac{\partial w_a}{\partial t} + u_a \frac{\partial w_a}{\partial x} + w_a \frac{\partial w_a}{\partial z} \right) = - \frac{\partial p_a}{\partial z} \quad (9)$$

where  $u_a$  and  $w_a$  are the horizontal and vertical components of the velocity,  $p_a$  is the pressure, and  $\rho_a$  is the density.

Boundary conditions supplement the equations (1) – (5) and (8) – (9). At the free interface located at  $z = h_o(1+h)$ , the application of the kinematic condition implies

$$w = \frac{\partial h}{\partial t} + U_o \frac{\partial h}{\partial x} + u \frac{\partial h}{\partial x} \quad \text{and} \quad w_a = \frac{\partial h}{\partial t} \quad (10)$$

The normal stress condition yields the relation between the liquid and air pressures and the interface shape.

$$-p + p_a = \sigma \frac{\partial^2 h}{\partial x^2} \left/ \left[ 1 + \left( \frac{\partial^2 h}{\partial x^2} \right)^2 \right]^{3/2} \right. \quad (11)$$

where  $\sigma$  is the coefficient of surface tension. At the centerline of the sheet,  $z = 0$ , either  $w = 0$  (symmetric case) or  $\frac{\partial w}{\partial z} = 0$  (anti-symmetric case) is imposed. Far away from the sheet,  $u_a \rightarrow 0$ ,  $p_a \rightarrow 0$ , and  $w_a \rightarrow 0$ .

When length, time, velocity, density, and pressure are scaled by  $h_0$ ,  $h_0/U_0$ ,  $U_0$ ,  $\rho_o$ , and  $\rho_o U_o^2$ , the following dimensionless system is obtained. The system has been linearized about the planar interface located at  $z = 1$ ,

$$\frac{\partial \rho}{\partial t} + \frac{\partial \rho}{\partial x} + \frac{\partial u}{\partial x} + \frac{\partial w}{\partial z} = 0 \quad (12)$$

$$\frac{\partial u}{\partial t} + \frac{\partial u}{\partial x} = -\frac{\partial p}{\partial x} \quad (13)$$

$$\frac{\partial w}{\partial t} + \frac{\partial w}{\partial x} = -\frac{\partial p}{\partial z} \quad (14)$$

$$\frac{\partial u_a}{\partial t} = -Q^{-1} \frac{\partial p_a}{\partial x} \quad (15)$$

$$\frac{\partial w_a}{\partial t} = -Q^{-1} \frac{\partial p_a}{\partial z} \quad (16)$$

$$\frac{\partial u_a}{\partial x} + \frac{\partial w_a}{\partial z} = 0 \quad (17)$$

with boundary conditions,

$$w = \frac{\partial h}{\partial t} + \frac{\partial h}{\partial x}, \quad w_a = \frac{\partial h}{\partial t} \quad \text{at } z = 1 \quad (18)$$

$$-p + p_a = We^{-1} \frac{\partial^2 h}{\partial x^2} \quad \text{at } z = 1 \quad (19)$$

$$w = 0 \text{ or } \frac{\partial w}{\partial z} = 0 \quad \text{at } z = 0 \quad (20)$$

$$u_a \rightarrow 0, \quad p_a \rightarrow 0, \quad \text{and } w_a \rightarrow 0 \quad \text{as } z \rightarrow \infty \quad (21)$$

where  $Q = \frac{\rho_a}{\rho}$  and  $We = \frac{h_o \rho_o U_o^2}{\sigma}$  are the density ratio and Weber number, respectively.

Gavzilyuk and Teshukov [9] have shown that in the linear regime, the effect of the vapor phase is described by a relationship between the pressure in the liquid phase and the density of the mixture as,

$$p = \alpha^2 \rho + \beta^2 \left( \frac{\partial}{\partial t} + \frac{\partial}{\partial x} \right)^2 \rho \quad (22)$$

where  $\alpha^2 = \frac{a^2}{U_o^2}$ , the term,  $a$ , being the speed of sound in the bubbly fluid, and  $\beta^2$  representing the characteristic length scale  $R/A_i$ ,  $A_i$  being the bubbles' interfacial area. For a fluid sheet moving at  $\sim 100$  m/s,  $a \sim 100$  m/s and  $\alpha^2 = O(1)$ .

On introducing the potential functions,  $\phi$  and  $\phi_a$  defined by

$$u = \phi_x, \quad w = \phi_z, \quad (\phi_a)_x = u_a, \quad (\phi_a)_z = w_a; \quad (23)$$

the governing system reduces to

$$\frac{\partial \rho}{\partial t} + \frac{\partial \rho}{\partial x} + \nabla^2 \phi = 0 \quad (24)$$

$$p = -\frac{\partial \phi}{\partial t} - \frac{\partial \phi}{\partial x} \quad (25)$$

$$p = \alpha^2 \rho + \beta^2 \left( \frac{\partial}{\partial t} - \frac{\partial}{\partial x} \right)^2 \rho \quad (26)$$

$$\nabla^2 \phi_a = 0 \quad (27)$$

$$p_a = -Q \frac{\partial \phi_a}{\partial t} \quad (28)$$

$$\frac{\partial \phi}{\partial z} = \frac{\partial h}{\partial t} + \frac{\partial h}{\partial x}, \quad \frac{\partial \phi_a}{\partial z} = \frac{\partial h}{\partial t} \quad \text{at } z = 1 \quad (29)$$

$$-p + p_a = We^{-1} \frac{\partial^2 h}{\partial x^2} \quad (30)$$

$$\frac{\partial \phi}{\partial z} = 0 \quad (\text{varicose}) \text{ or } \phi = 0 \quad (\text{sinuous}) \text{ or at } z = 0 \quad (31)$$

$$\phi_a \rightarrow 0, \quad \text{and } p_a \rightarrow 0 \quad \text{as } z \rightarrow \infty \quad (32)$$

Equations (25) and (26) imply,

$$-\alpha^2 \rho - \beta^2 \left( \frac{\partial}{\partial t} + \frac{\partial}{\partial x} \right)^2 \rho = \left( \frac{\partial}{\partial t} + \frac{\partial}{\partial x} \right)^2 \phi \quad (33)$$

By operating with  $\left( \frac{\partial}{\partial t} + \frac{\partial}{\partial x} \right)$  on both sides of equation (33) and on using equation (24), we find,

$$\alpha^2 \nabla^2 \phi + \beta^2 \left( \frac{\partial}{\partial t} + \frac{\partial}{\partial x} \right)^2 \nabla^2 \phi = \left( \frac{\partial}{\partial t} + \frac{\partial}{\partial x} \right)^2 \phi \quad (34)$$

The analysis of the system consisting of equations (34), (27), and (28) and boundary conditions given by equations (29) – (32) using the Fourier transform,  $\phi = \hat{\phi}(z) \exp(\omega t + ikx)$ , yields the following dispersion relation,

$$k(\omega + ik)^2 \coth(l) + Ql\omega^2 = -lRk^3 \quad (35)$$

for the varicose mode, and

$$k(\omega + ik)^2 \tanh(l) + Ql\omega^2 = -lRk^3 \quad (36)$$

for the sinuous mode, where

$$l = \left[ k^2 + \frac{(\omega + ik)^2}{\alpha^2 + \beta^2(\omega + ik)^2} \right]^{1/2} \quad (37)$$

and  $\omega$  and  $k$  are the growth rate and the wavenumber, respectively.

Analysis of the dispersion relations:

The term  $(\omega + ik)^2 / [\alpha^2 + \beta^2(\omega + ik)^2]$  in Eq. (37) determines the influence of the presence of bubbles on the onset of instability. The stability characteristics can be determined directly by solving the dispersion relation, equations (35) and (36), for the growth rate  $\omega$  as function of the wavenumber  $k$  for fixed values of the Weber number and the density ratio  $Q$ . This approach, however, does not yield a quantitative assessment of the wavelength of the instability. In order to isolate the main effects of the bubble's presence, we proceed as follows.

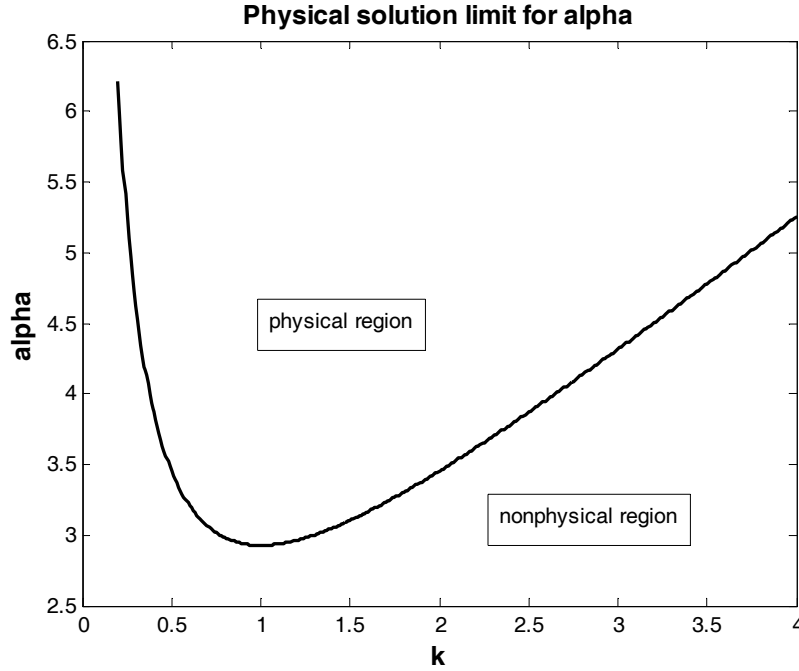


Figure 1. Plot of the line where  $l$  equals zero as a function of  $k$  and  $\alpha$ . The parameters  $Q$ ,  $\beta$ , and  $b$  are set to 0.001, 1.0, and 1.0, respectively. When  $l$  is complex, the dispersion relations, equations (35) and (36), are nonphysical. When  $l$  is real, the dispersion relation equations can yield physical information about the neutral stability curve.

At the onset of instability, the real part of  $\omega$  is zero. Let  $\omega = ib$ , where  $b$  is the frequency of oscillations at onset. If  $b$  happens to be zero as well, then the instability becomes a steady mode. On setting  $\omega = ib$  in equations (35), (36), and (37), we obtain

$$-k(b+k)^2 \frac{\coth(l^*)}{l^*} - Qb^2 = -Rk^3 \quad (38)$$

and

$$-k(b+k)^2 \frac{\tanh(l^*)}{l^*} - Qb^2 = -Rk^3 \quad (39)$$

where

$$l^* = \left[ k^2 - \frac{(k+b)^2}{\alpha^2 - \beta^2(k+b)^2} \right]^{1/2} \quad (40)$$

Generally, the expression for  $l^*$  is complex. On letting  $l^* = \mu + iv$ , so

$$\frac{\tanh(l^*)}{l^*} = \frac{\tanh(\mu + iv)}{(\mu + iv)} = p + iq \quad (41)$$

Equating the real and imaginary parts of the dispersion relation for the varicose mode implies that

$$k(b+k)^2 p + Qb^2 = +Rk^3 \quad (42)$$

and

$$kq(b+k)^2 = 0 \quad (43)$$

For a non-zero wave number, the imaginary part clearly implies that  $q = 0$ . A similar argument also yields  $q = 0$  for the sinuous mode; ie, the expression for  $l^*$  is real. The region in the parameter space of the problem where  $l^*$  is real is termed the physical region, and a representative case is depicted in figure 1.

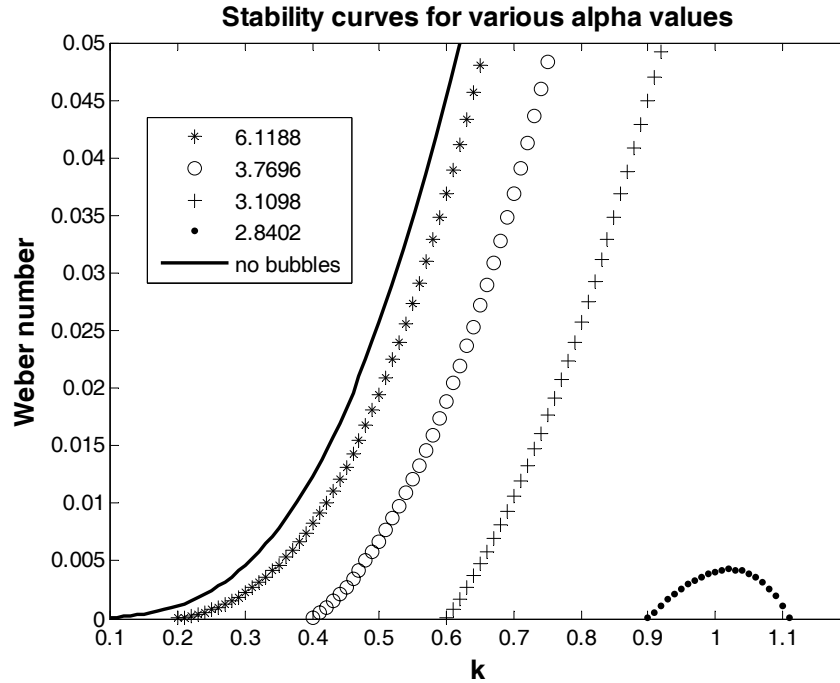


Figure 2. Plots of a neutral stability curve for a purely liquid sheet (“no bubbles”) in a gas and of neutral stability curves for liquid sheets, with various concentrations of bubbles as indicated by the values of  $\alpha$ , in a gas. The sheet’s interface deformation is varicose. The parameters  $Q$ ,  $\beta$ , and  $b$  are set to 0.001, 1.0, and 1.0, respectively.

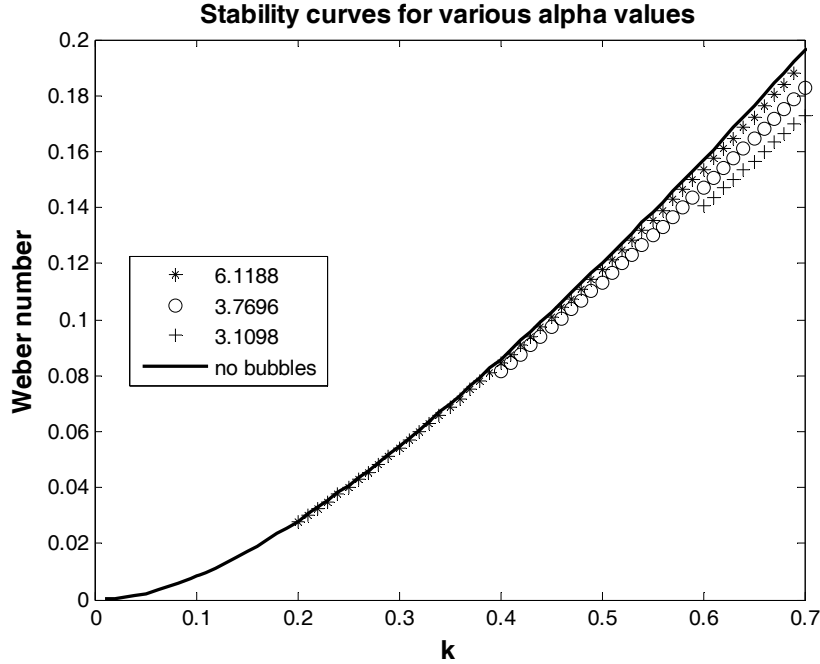


Figure 3. Plots of a neutral stability curve for a purely liquid sheet and for bubbly sheets. Conditions are the same as in figure 1 except for the mode. The sheet's interface deformation is sinusous.

Equation (42) yields the expression for the Weber number, namely

$$We = \frac{k^3}{k(b+k)^2 p + Qb^2} \quad (44)$$

where  $p$  is the real part of  $\frac{\coth(l^*)}{l^*}$ . This expression for the Weber number is valid for any non-zero value of the frequency  $b$ . The non-vanishing  $b$  is expected, based on physical grounds. The determination of  $b$  is not carried out here.

Equation (44) depicts the dependence of the Weber number on the wavenumber,  $k$ , the oscillation frequency,  $b$ , the density ratio,  $Q$ , and the parameter  $p$  which incorporates the effect of the air bubbles.

Figure 1 illustrates the division of the  $\alpha$ - $k$  space into physical and nonphysical regions when  $\beta$  is set to 1.0,  $b$  to 1.0 and  $Q$  to 0.001. These parameters describe a sheet of liquid water moving through air.

A plot of equation (38) versus  $k$ , for a set of parameters that is physically realizable according to figure (1), is shown in figure (2).

Equations (38) for the varicose mode and its equivalent for the sinuous mode can be readily solved to yield neutral stability curves for various values of  $\alpha$  as a function of the wave and Weber numbers.

Figure 2 illustrates the neutral stability curves that describe the varicose mode for the parameter combination used to plot the figure 1. The solid line describes a liquid sheet containing no vapor bubbles. The interaction between the purely liquid sheet and a gas has been described by Senecal et al. [1] who explain that as the wavenumber decreases, the Weber number for sheet instability decreases to the limit of zero Weber number for zero wavenumber.

As explained above, for low concentration of bubbles the increase of bubble concentration to the liquid sheet increases the mixture's compressibility which subsequently decreases the sound speed in the mixture. In figure 2, therefore, smaller values of  $\alpha$  correspond to larger bubble concentrations. In general the effect of increasing bubble concentration seems to lower the neutral stability curve. A small bubble concentration necessary to yield a nondimensional sound speed to 6.1188 causes the neutral stability curve to fall slightly below the "no bubbles", or purely liquid, case. The smallest value of  $\alpha$  studied indicates that when  $\alpha$  decreases to 2.8402, the flow is unstable until the wavenumber reaches 0.9 and can be stable near this wavenumber only for Weber numbers less than 0.004.

Figure 3 is included to illustrate the effect of bubble concentration on the stability of a liquid sheet with a sinuous deformation. As indicated by the solid line in figure 3, the purely liquid is more stable in the sinuous mode. Bubble concentration, likewise, has a much smaller effect on the neutral curve than it does for the varicose mode.

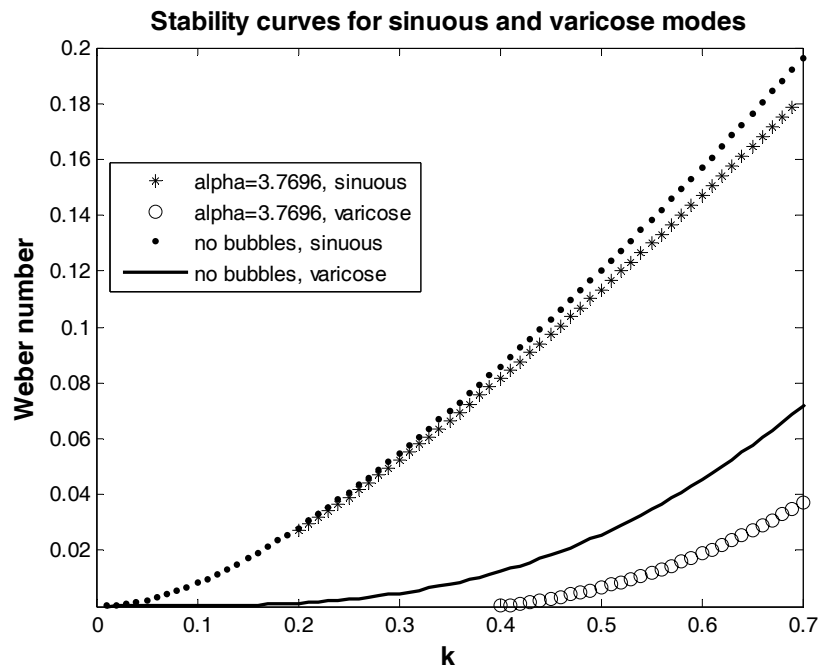


Figure 4. Plots comparing the sinuous and varicose neutral stability curves for the purely liquid sheets and for two-phase sheets.

In figure 4, a comparison is made between varicose and sinuous mode neutral stability curves. Of the two modes for purely liquid sheets, the varicose mode is seen to be considerably less stable. When the sheet is two-phase such that  $\alpha$  is 3.77, the sheet in either mode is less stable than the purely liquid sheet. The effect of bubble addition, however, is considerably greater when the sheet's interface is varicose.

Finally, the effect of the density ratio  $Q$  was studied. When  $Q$  was increased by an order of magnitude over that used for the plots in figures 2 and 3, no noticeable effect of the neutral stability curves could be discerned either for the varicose or the sinuous modes.

## Conclusions

The breakup of a bubbly inviscid liquid sheet has been analyzed. A bubbly liquid model has been considered for which the stability analysis is mathematically tractable yet which contains the main physical ingredients caused by the presence of the bubbles, including the coupled effect of the volume fraction of bubbles and compressibility. The speed of sound in the bubbly mixture appears as an important parameter in the model. The results indicate that the presence of the bubbles does not alter the threshold for the onset of instability. Within the model's assumptions, the sheet is unstable at zero wavenumber, with or without the presence of bubbles. In the pure liquid case, instability initiates at zero wavenumber; however, any level of bubble concentration, albeit very small, modifies the critical wavenumber. If the size of the droplets upon sheet breakup is correlated with the critical wavelength, then the presence of bubbles would act in such a way as to produce smaller size liquid droplets.

## Nomenclature

$a$	speed of sound
$A_i$	density of bubbles' interface area
$b$	complex part of growth function
$h$	location of interface in z-direction
$k$	wave number
$l$	expression defined in paper
$l^*$	expression defined in paper
$N$	number of bubbles per volume
$p$	pressure
$Q$	ratio of gas density to sheet density
$R$	bubble radius
$t$	time
$u, w$	velocity components
$x, z$	spatial coordinates
$w$	y-velocity component
	$\frac{h_o \rho_o u_o^2}{\sigma}$
$We$	Weber number, $\frac{\sigma}{\rho_o u_o^2}$
$\alpha$	speed of sound scaled with $u_o$
$\beta$	characteristic length scale
$\phi$	potential function
$\gamma$	polytropic gas exponent
$\rho$	density
$\sigma$	surface tension
$\omega$	growth function (complex)

## Subscripts

$a$	gas surrounding sheet
$g$	vapor
$l$	liquid
$o$	equilibrium

## References

- Senecal, P.K., D.P. Schmidt, I. Nouar, C.J. Rutland, R.D. Reitz, and M.L. Corradini, *International Journal of Multiphase Flow*, 25, 1073 – 1097, (1999).
- Brennen, C.E., *Cavitation and Bubble Dynamics*, Oxford, 1995, p. 166.
- Karplus, H.B., Illinois Inst. Tech. Rep. COO-248, (1958)
- Gouse, S.W. and Brown, G.A., ASME Paper 64-WA/FE - 35, (1964).
- Sirignano, W.A. and C. Mehring, *Progress in Energy and Combustion Science*, 26, 609 – 655, (2000).
- Kogarko, B.S., *Dokl. AN SSSR*, 137, 1331 – 1333, (1961).
- Iordanski, S.V., *Zhurnal Prikladnoj Mekhanikii Tekhnicheskoy Fiziki*, N3, 102 – 111, (1960)
- van Wijngaarden, L., *Ann. Rev. Fluid Mech.*, 4, 369 – 396, (1972).
- Gavrilyuk, S.L. and V.M. Teshukov, *Studies in Appl. Math.*, 113, 1 – 29, (2004)